This article has been accepted for publication in a future issue of this journal, but has not been fully edited. Content may change prior to final publication. Citation information: DOI 10.1109/LMAG.2016.2592462, IEEE Magnetics Letters

# Curie Temperature Engineering in High Entropy Alloys (HEAs) for Magnetocaloric Applications

Michael Kurniawan[1], Alice Perrin[1], Patricia Xu[1], Vladimir Keylin[1], and Michael McHenry[1*]

[1] *Department of Materials Science and Engineering, Carnegie Mellon University, Pittsburgh, PA 15213, USA*

[*] *Senior Member, IEEE*

Corresponding author: M. Kurniawan (mkurniaw@andrew.cmu.edu)

## Abstract

High entropy alloys (HEAs) have attracted recent attention for applications requiring high strength, oxidation resistance, and high temperature stability. HEAs used in magnetocaloric applications have also been reported. The majority of reports on magnetocaloric applications using HEAs focus on increasing the refrigeration constant (RC) and engineering the Curie temperature ($T_c$). Herein, we investigate the role of alloy additions; (a) noble metals (e.g. Cu, Ag), (b) antiferromagnetic transition metals (e.g. Mn), (c) Stoner-enhanced transition metals (e.g. Pt), and (d) early transition metals (e.g. Mo) that contribute to the virtual bound states (VBS); on exchange interaction distributions when added to base alloys with equiatomic ferromagnetic late transition metals (Fe, Co, and Ni). We demonstrate the ability to; (1) stabilize a ferromagnetic fcc γ-phase with equiatomic compositions in 4-, 5- and 6-component systems, (2) make slight departures from equiatomic compositions to a chosen alloy to bring its $T_c$ nearer to room temperature, and (3) measure the role of alloying on exchange interaction distributions. We present a simple model to predict $T_c$ in HEAs using the Bethe-Slater curve and binary

phase diagrams of alloy constituents. Compared to the rare earth-based magnetocaloric materials, the HEAs investigated here have significantly lower costs.

***Index Terms*** *– Magnetocaloric effect, Curie temperature, high entropy alloys, magnetic materials.*

# Introduction

High entropy alloys (HEAs) are multicomponent alloy systems where the configurational entropy is larger than the fusion entropy of most common metals. In many HEA systems, simple BCC or FCC constituent phases can be entropically stabilized instead of forming intermetallics [Cantor 2004, Cantor 2007, Varalakshmi 2010, Senkov 2011, Lin 2010]. Many HEAs are studied for enhanced solid solution strengthening and resistance to softening. These mechanical properties make them attractive for high temperature applications. In certain systems, several of the components are ferromagnetic transition metals where interesting magnetic properties may also be derived [Lucas 2013].

The magnetic properties of 4-component FeNiCoCr-based HEAs have been reported by several groups [Yeh 2004]. Wang *et al*. presented M-H curves at room temperature for as-cast FeCoNiCuCr and FeCoNiCuCrAl [Wang 2009]. Zhang *et al*. reported M-H curves at room temperature and M-T curves from 100-350 K in as cast and annealed FeCoNiCuCrAl alloys [Zhang 2010]. Lucas *et al*. measured high temperature M-T and showed that Pd additions increase the Curie temperature ($T_c$) of FeNiCoCr from below room temperature to 440 K for FeNiCoCrPd and to 503 K for $FeNiCoCrPd_2$

This article has been accepted for publication in a future issue of this journal, but has not been fully edited. Content may change prior to final publication. Citation information: DOI 10.1109/LMAG.2016.2592462, IEEE Magnetics Letters

[Lucas 2011]. Here, we extend studies of nominally equiatomic 4-component systems to 5-component systems while providing a framework for understanding distributed exchange interactions in these alloy systems and their role in the peak entropy and $T_c$ in near room temperature magnetocaloric materials. This is achieved through control of the chemical distribution of exchange bonds in the system, as well as by studying small departures from equiatomic compositions aimed at tuning $T_c$ to near room temperature.

The magnetocaloric effect (MCE) refers to the temperature change of a magnetic material on application of a magnetic field (H) in adiabatic condition. MCE is also known as adiabatic demagnetization. With increasing H, the entropy of the spin subsystem is reduced and is balanced by an increase in lattice entropy under adiabatic conditions. Increased lattice entropy causes heating of the material [Franco 2006]. MCE based refrigeration devices have been recently announced for adoption in consumer products [General Electric 2014]. MC materials are interesting for magnetic refrigeration near room temperature, because the technology is 20% more efficient than gas compression refrigeration [Gschneidner 2000]. MCE can also contribute to passive cooling to control heating in power conversion applications where temperature rise due to losses is a limiting factor in magnetic components for high frequency power electronics [Leary 2012]. Recent MCE research has focused on materials for room-temperature applications with high efficiency, low cost and reduced reliance on strategic rare-earth elements [Ucar 2012, Ucar 2014, Eggert 2011, Hurd 2012]. To achieve this goal, transition metal systems have been investigated to replace rare-earth metals for cost reduction. γ-Fe-Ni alloys are economical alternatives with refrigeration coefficients (RC) that can be tuned by alloying and the breadth of the magnetic transition can be controlled

by impurity and positional disorder-derived distributed exchange interactions [Ucar 2014, Jones 2012, Gallagher 1999, Ucar 2013, Ipus 2012]. Ternary γ-Fe-Co-Ni alloys are equally possible but with higher $T_c$ of less technological relevance for room temperature MCE. However, quaternary and quinternary Fe-Co-Ni-based alloys may be of considerable interest to the extent that distributed exchange interactions allow for tunable $T_c$ and better control of RC through distribution of magnetic and non-magnetic species on a template lattice with attention to the nature of the exchange bonds between the constituents.

HEAs offer a test-bed for studying distributed exchange interactions in systems with well defined crystalline positions. Here we consider 5-component equiatomic (1) FeCoNiCuMn, (2) FeCoNiCuAg and (3) FeCoNiCuPt and (4) FeCoNiCuMo alloys. Equiatomic compositions are chosen to maximize configurational entropy. It is of course a rational alloy design approach to further tune the compositions toward an engineering goal of tuning the $T_c$ to a specific value. However, this scientific approach is aimed at comparing 5-component systems with different exchange bonds on an equal footing. In the most promising alloys slight departures from equiatomic compositions can be made to realize more precise $T_c$ tuning.

In all four systems, there exist Ni-Ni, Ni-Co, Ni-Fe, Co-Co, Co-Fe and Fe-Fe direct exchange interactions between the elemental ferromagnetic components. The exchange interactions are further distributed due to weaker second and larger nearest neighbor interactions [MacLaren 1999]. Cu is a non-magnetic transition metal component of comparable size that acts as a diluent with negligible or weak RKKY coupling to the ferromagnetic components. Similar to Cu and Au, Ag is a non-magnetic transition metal

This article has been accepted for publication in a future issue of this journal, but has not been fully edited. Content may change prior to final publication. Citation information: DOI 10.1109/LMAG.2016.2592462, IEEE Magnetics Letters

but slightly larger [McHenry 1991, McHenry 1990, MacLaren 1990]. Cu and Ag components serve to reduce the alloy $T_c$ by simple dilutional effects with only slight contact polarization [McHenry 1990]. In alloy (1), there are additional Mn-Ni, Mn-Co, Mn-Fe and Mn-Mn interactions, which at nearest neighbor distances are antiferromagnetic. Because of negative antiferromagnetic interactions in these systems, the distribution of exchange interactions is broader than in alloys for which simple dilutional substitutions are made. The broader distribution of exchange interactions also results in a large low temperature tail. Antiferromagnetic exchange interaction also exists in Cr-containing systems.

In alloy (2), two non-magnetic diluents, Cu and Ag are used to further tune the $T_c$. In alloy (3), the non-magnetic diluent, Ag, is replaced by Pt, which like Pd is a Stoner-enhanced metal [MacLaren 2001, Willoughby 2002, Willoughby 2003], for which it is well known that the contact potential with Fe, Co and Ni gives rise to local moment formation and therefore additional weak Pt-Ni, Pt-Co, and Pt-Fe direct exchange interactions [McHenry 1991]. Other Stoner-enhanced metals include Ru and Rh. In alloy (4), the second diluent is replaced by Mo for which the relative valence difference $\Delta Z > 2$ with respect to all three of the ferromagnetic transition metals and Cu, and therefore contributes virtual bound states (VBS) [Corb 1985, Ghemawat 1989] with moment reductions as predicted by Friedel [Friedel 1958]. The effect of these additions is to change the shape of the transition metal bands because of the strong perturbing potential of a non-magnetic species. The d-d hybrid bonding between the early and magnetic transition metals, and VBS rob the electrons from the polarizable transition metal d-states as well as change the shapes of the transition metal band shapes [O'Handley 1987]. The

first effect is dilutional, while the second alters the Ni-Ni, Ni-Co, Ni-Fe, Co-Co, Co-Fe and Fe-Fe direct exchange interactions in a way only predictable from band theory. Magnetic moment variation in such systems has been systematically described in terms of magnetic valence ideas [Williams 1988]. In general, early transition metals (e.g. Mo, V, Nb, Ti) can dramatically reduce the magnetization and lower the $T_c$ in such systems. Substitutional solid solutions with these species are limited by intermetallic phase formation, most notably Frank-Kaspar and Lave's phases. Mn and Mo are known to be γ-stabilizers in Fe. RKKY mediated exchange interaction exists in rare earth-based magnetocaloric materials but is not discussed since all HEAs in this work are rare earth-free.

## Experimental Procedures

Ingots with nominal equiatomic compositions FeCoNiCuMn, FeCoNiCuAg, FeCoNiCuPt and FeCoNiCuMo were prepared from high purity elements by Mini Arc Melting System MAM-1 (Edmund Buhler GmbH), in Argon atmosphere [McHenry 1999]. Rapidly quenched irregular shape nanocomposite flakes were prepared from the ingots by SC Melt Spinner (Edmund Buhler GmbH) in low-pressure Argon atmosphere (300 mBar abs.), with Boron Nitride crucible and nozzle of 1.5 mm diameter orifice, using copper quenching wheel with 40 m/s circumferential speed [McHenry 1999].

As-cast samples were characterized by X-ray diffraction (XRD) using a Philips X'Pert multipurpose diffractometer working in continuous scanning mode with Cu Kα radiation ($\lambda = 0.1541874$ nm). Lattice parameters were calculated using the Nelson-Riley method [Nelson 1945]. Crystallite sizes were estimated from XRD peak breadths using a

standard Scherrer analysis, assuming only crystallite size broadening. Electron dispersive spectroscopy (EDS) on an ASPEX Express scanning electron microscope (SEM) was used for chemical mapping on the HEA samples in this work.

The magnetization versus temperature curve was obtained using the Vibrating Sample Magnetometer (VSM) function in a Quantum Design Physical Property Measurement System (PPMS). The applied field (H) ranges from 0 to 480 kA/m, with an interval of 16 kA/m. The measurement was carried out in the temperature range near $T_c$ of respective alloys, with an interval of 10 K.

## Results and Discussion

XRD patterns of all as-cast samples show diffraction peaks corresponding to a simple FCC solid solution phase (**Fig. 1(e)**). Compared to FeCoNiCuMn and FeCoNiCuPt, FeCoNiCuAg and FeCoNiCuMo exhibit broader XRD peaks (e.g. [111], [200] and [311]) and several additional peaks ($2\theta = 38^o$, $65^o$, and $78^o$).

FIG 1 HERE

For the compositions with a simple FCC phase shown in **Fig. 1**, area scan EDS images were taken on an ASPEX Express SEM to confirm that the compositions throughout the materials were homogeneous. Area scan EDS map of each composition was taken at various points in each sample to ensure that the results were representative of the sample.

The area scans EDS of the FeCoNiCuMn and FeCoNiCuPt samples (**Fig. 1(a)** and

This article has been accepted for publication in a future issue of this journal, but has not been fully edited. Content may change prior to final publication. Citation information: DOI 10.1109/LMAG.2016.2592462, IEEE Magnetics Letters

**Fig. 1(c)**) show that the samples are homogeneous, while those of FeCoNiCuAg and FeCoNiCuMo samples (**Fig. 1(b)** and **Fig. 1(d)**) show imhomogeneity. In the FeCoNiCuAg sample, there seems to be an AgCu phase, while the FeCoNiCuMo sample seems to have Cu rich crystals throughout the sample. The EDS results suggest that these samples are not made of a single FCC solid solution phase, but of multiple FCC phases. The SEM data here corroborates XRD data (**Fig. 1(e)**), which indicates small amounts of second phase intermetallics present in FeCoNiCuAg and FeCoNiCuMo alloys. Since both Ag and Mo are slightly larger than Fe, Co, Ni, and Cu, simple Hume-Rothery rules predict the higher proclivity for intermetallic formation in these systems [Cahn 1996].

The magnetization curves of all samples are shown in **Fig. 2**, showing $T_c$ values ranging from 400 K to above 1000 K. FeCoNiCuAg and FeCoNiCuMo exhibit irreversible M-T curves during the heating-cooling cycle, in agreement with the EDS area scan data (**Fig. 1**) that show chemical partitioning in these systems. FeCoNiCuMn has the lowest $T_c$ at 400 K among all others, while FeCoNiCuAg has the highest $T_c$ of >1000 K, which is beyond our measurement limit. The addition of Mn to FeCoNiCu results in the decrease of $T_c$ from >1000 K to near the boiling temperature water. A dramatic reduction of $T_c$ was also observed with the addition of Cr to FeCoNiCu, with FeCoNiCuCr exhibiting $T_c$ of 130 K (not shown). Both Mn and Cr form antiferromagnetic exchange bonds with Fe, Co, and Ni. In FeCoNiCuMn, antiferromagnetic Fe-Mn, Co-Mn, Ni-Mn, Mn-Mn bonds are present.

Ag has been reported to be immiscible in multicomponent FCC in several HEAs due to its larger atomic size than Fe, Co, and Ni [McHenry 1991, McHenry 1990, MacLaren 1990]. While not as expensive as Au, the price of Ag is relatively more

expensive than elements such as Fe, Co, Ni, Cu, and Mn [www.metalprices.com, www.metal-pages.com]. As seen from **Fig. 2**, the dilution effect of Ag is insufficient to lower down the $T_c$ of FeCoNiCu to ambient temperature. In our measurement, the $T_c$ of FeCoNiCuAg is above 1000 K, which is the upper limit of the PPMS in our facility.

Among these four HEAs, FeCoNiCuPt exhibits the highest specific magnetization (σ) at 64.24 $A.m^2/kg$, while FeCoNiCuMo is the lowest at 15.28 $A.m^2/kg$. In the former, there are additional weak Fe-Pt, Co-Pt, and Ni-Pt exchange interaction due to the contact potential. This is a well-known behavior in Stoner-enhanced metals (e.g. Ru, Rh, Pd, and Pt) [MacLaren 2001, Willoughby 2002, Willoughby 2003]. The uses of these elements in future HEA applications must, however, account for their high price, which will inevitably increase the alloy costs [www.metalprices.com, www.metal-pages.com, Kurniawan 2015, Kurniawan 2015]. In systems consisting of early transition metals such as Mo, V, Nb, and Ti, VBS rob the electrons from the polarizable d-states. This results in a large decrease of $T_c$ and magnetization in FeCoNiCuMo.

FIG 2 HERE

Magnetization isotherms (**Fig. 3**) were obtained by performing isothermal M-H in appropriate temperature ranges. By integrating the differential ΔM/ΔT from 0 to 480 kA/m, ΔS-T curves were obtained. The calculation to arrive at ΔS–T curve follows (1);

$$\Delta S\ (T) = \sum_{H=\ 0\ kA/m}^{H=\ 480\ kA/m} \left\{ \left( \frac{\Delta M}{\Delta T} \right)_H \times \Delta H \right\} \quad (1)$$

FIG 3 HERE

The reduction in magnetization of FeCoNiCuMo due to the formation of VBS also results in a small ΔS–T peak value. The most promising HEA investigated here is FeCoNiCuMn, with $T_c$ slightly higher than room temperature. Fine-tuning the alloy to achieve a $T_c$ close to room temperature may require slight deviation from equiatomic composition [Belyea 2015].

In HEAs, we seek to stabilize solid solutions by leveraging the configurational entropy of multicomponent alloys. When the number of constituents is large enough, the bonding enthalpy can be overcome and stable solid solutions are achieved. As summarized in **Table I**, by having larger number of constituents, higher configurational entropy is increased significantly. Another interesting point to mention is the small change in configurational entropy when deviating from equiatomic composition. By going from equiatomic FeCoNiCuMn to $FeCoNiCu_{0.75}Mn_{1.25}$, the change is configurational entropy is less than 1%. This value is small compared to the change in configurational entropy when more constituents are added to the alloy (>11%).

TABLE I HERE

A simple $T_c$ prediction on equiatomic FeCoNiCu alloy can be made if the $T_c$ and (x, y) coordinate (in the Bethe-Slater curve) of each individual element are known. This method averages the exchange interactions among all the atomic constituents of a HEA. On the Bethe-Slater curve, x and y coordinates denote interatomic distance and exchange

integral, respectively [McHenry 1999]. In an equiatomic alloy, there is an equal number of each possible bond, and the exchange energy of each bond can be substituted into (2) to estimate $T_c$.

$$T_c = \frac{2ZJ_{ex}S(S+1)}{3K_B} \quad (2)$$

In **Table II**, we compare calculated and measured $T_c$ of several HEAs with 4, 5, and 6 components. Lastly, based on this averaged exchange interaction method, we also made a prediction for the $T_c$ of FeCoNiCuMnPt alloy to be close to ambient temperature.

This method was limited due to the number of non-ferromagnetic binary combinations of elements in each alloy for which a $T_c$ could not be obtained; because of this, we could not calculate the $T_c$ for FeCoNiCuAg and FeCoNiCuMo with this method alone. However, these alloys as well as future alloys can be assessed using a similar method with exchange energies estimated by spin-polarized relativistic Korringa-Kohn-Rostoker (SPRKKR) software, and the values in the table for FeCoNiCuAg and FeCoNiCuMo were calculated using this software [Ebert 2011].

TABLE II HERE

Among the alloys we examined (**Table II**), FeCoNiCuMn and FeCoNiCuMnPt have $T_c$ closest to ambient temperature. However, since the high price of Pt will undoubtedly increase the total alloy cost of FeCoNiCuMnPt, we are interested in exploring FeCoNiCuMn further. As seen in **Table I**, the configurational entropy of FeCoNiCuMn decreases negligibly with slight deviations from equiatomic composition. However, a small change in the relative amounts of Cu and Mn in FeCoNiCuMn results

in substantial shift in its $T_c$. As shown in **Table III**, $FeCoNiCu_{0.95}Mn_{1.15}$ exhibits $T_c$ of 265 K, which deems this system to be suitable for MC applications near ambient temperature.

TABLE III HERE

**Fig. 4** shows the M-T and ΔS–T curves of FeCoNiCuMn, $FeCoNiCu_{0.95}Mn_{1.05}$, and $FeCoNiCu_{0.90}Mn_{1.10}$, with $T_c$ of 400, 280, and 265 K, respectively. Based on our XRD and SEM measurement on these alloys, no chemical partitioning was observed and thus only FCC solid solutions were present. Thus, by this simple fine-tuning of the alloy composition, one does not compromise on the structural stability of the HEAs, while the $T_c$ and RC can be engineered favorably.

FIG 4 HERE

## Acknowledgments

M. K and M. E. M acknowledge support of the NSF through Grant No. DMR #0804020.

## References

Cantor B, Chang I T H, Knight P, Vincent A J B (2004), "Microstructure development in equiatomic multicomponent alloys", *Mater. Sci. Eng. A,* 375, 213–218.

Cantor B (2007), "Stable and metastable multicomponent alloys", *Ann. Chim. Sci. Mater,* 32, 245–256.

Varalakshmi S, Kamaraj M, Murty B S (2010), "Processing and properties of nanocrystalline CuNiCoZnAlTi high entropy alloys by mechanical alloying", *Mat. Sci. Eng. A*, 527(4), 1027-1030.

Senkov O N, Scott J M, Senkova S V, Miraclea D B, Woodward C F (2011), "Microstructure and room temperature properties of a high-entropy TaNbHfZrTi alloy", *J. Alloy Compd*., 509(20), 6043-6048.

Lin C M, Tsai H L, Bor H Y (2010), "Effect of aging treatment on microstructure and properties of high-entropy $Cu_{0.5}$CoCrFeNi alloy", *Intermetallics*, 18(6), 1244-1250.

Lucas M S, Belyea D, Bauer C, Bryant N, Michel E, Turgut Z, Leontsev S O, Horwath J, Semiatin S L, McHenry M E, Miller C W (2013), "Thermomagnetic analysis of $FeCoCr_xNi$ alloys: magnetic entropy of high-entropy alloys", *J. Appl. Phys*., 113, 17A923.

Yeh J W, Chen S K, Lin S J, Gan J Y, Chin T S, Shun T T, Tsau C H, Chang S Y (2004), "Nanostructured high-entropy alloys with multiple principal elements: novel alloy design concepts and outcomes", *Adv. Eng. Mater*., 6(5), 299.

Wang Y P, Li B S, Fu H Z (2009), "Solid solution or intermetallics in a high-entropy alloy ", *Adv. Eng. Mater*., 11(8), 641.

Zhang K B, Fua Z Y, Zhanga J Y, Shib J, Wanga W M, Wanga H, Wanga Y C, Zhang Q J (2010), "Annealing on the structure and properties evolution of the CoCrFeNiCuAl high-entropy alloy", *J. Alloys Compd*., 502, 295.

Lucas M S, Mauger L, Muñoz J A, Xiao Y, Sheets A O, Semiatin S L, Horwath J, Turgut Z (2011), "Magnetic and vibrational properties of high-entropy alloys", *J. Appl. Phys*., 109, 07E307.

Franco V, Borrego J M, Conde C F, Conde A, Stoica M, Roth S (2006), "Refrigerant capacity of FeCrMoCuGaPCB amorphous alloys", *J. Appl. Phys*., 100, 083903.

http://www.geglobalresearch.com/innovation/magnetocaloric-materials-chill-next-generation-refrigerators.

Gschneidner K A, Pecharsky V K (2000), "Magnetocaloric materials", *Annu. Rev. Mater. Sci*., 30, 387–429.

Leary A M, Ohodnicki P R, McHenry M E (2012), "Soft magnetic materials in high-frequency, high-power conversion applications", *JOM*, 64, 772.

Ucar H, Ipus J J, Franco V, McHenry M E, Laughlin D E (2012), "Overview of magnetocaloric materials operating near room temperature", *JOM*, 64(7), 782-788.

Ucar H, Craven M, Laughlin D E, McHenry M E (2014), "The effect of Mo additions on structure and magnetocaloric effect in γ-FeNi nanoparticles", *J. Electron. Mater*., 43(1), 137-141.

Eggert R (2011), "Minerals go critical", *Nat. Chem.*, 3, 688-691.

Hurd A, Kelley R, Lee M, Eggert R (2012) "Energy-critical elements for sustainable development", *MRS Bull.*, 37 (4), 405-410.

Jones N J, Ucar H, Ipus J J, McHenry M E, Laughlin D E (2012), "The effect of distributed exchange parameters on magnetocaloric refrigeration capacity in amorphous and nanocomposite materials", *J. Appl. Phys.*, 111, 07A334.

Gallagher K A, Willard M A, Zabenkin V, Laughlin D E, McHenry M E (1999),

"Amorphous/nanocrystalline alloys-distributed exchange interactions and temperature dependent magnetization in amorphous $Fe_{88-x}Co_xZr_7B_4Cu_1$ alloys", *J. Appl. Phys*., 85(8), 5130.

Ucar H, Ipus J J, Laughlin D E, McHenry M E (2013), "Tuning the Curie temperature in γ-FeNi nanoparticles for magnetocaloric applications by controlling the oxidation kinetics", *J. Appl. Phys*., 113, 17A918.

Ipus J J, Herre P, Ohodnicki P R, McHenry M E (2012), "High temperature XRD determination of the BCC-FCC transformation temperature in $(Fe_{70}Ni_{30})_{88}Zr_7B_4Cu_1$ nanocomposites", *J. Appl. Phys*., 111, 07A323-07A325-27.

MacLaren J M, Schulthess T C, Butler W H, Sutton R A, McHenry M E (1999), "Electronic structure, exchange interactions, and Curie temperature of FeCo", *J. Appl. Phys*., 85, 4833-35.

McHenry M E, MacLaren J M (1991), "Iron and chromium monolayer magnetism in noble-metal hosts: systematics of local moment variation with structure", *Phys. Rev. B*, 43, 10611-16.

McHenry M E, MacLaren J M, Eberhart M E, Crampin S (1990), "Electronic and magnetic properties of Fe/Au multilayers and interfaces", *J. Magn. Magn. Mat.*, 88, 134–150.

MacLaren J M, McHenry M E, Crampin S, Eberhart M E (1990), "Magnetic and electronic properties of Au/Fe superlattices and interfaces", *J. Appl. Phys.*, 67, 5406-08.

MacLaren J M, Willooughby S A, McHenry M E, Ramalingum B, Sankar S G (2001), "First principles calculations of the electronic structure of $Fe_{1-x}Co_xPt$", *IEEE Trans. Mag*., 37, 1277 - 1279.

Willoughby S D, MacLaren J M, Ohkubo T, Jeong S, McHenry M E, Laughlin D E, Choi S J, Kwon S J (2002), "Electronic, magnetic, and structural properties of $L1_0$ $FePt_xPd_{1-x}$ alloys", *J. Appl. Phys*., 91,

8822-24.

Willoughby S D, Stern R A, Duplessis R, MacLaren J M, McHenry M E, Laughlin D E (2003), "Electronic structure calculations of hexagonal and cubic phases of $Co_3Pt$", *J. Appl. Phys*., 93, 7145-47.

McHenry M E, MacLaren J M, Clougherty D P (1991), "Monolayer magnetism of 3d transition metals in Ag, Au, Pd, and Pt hosts: systematics of local moment variation", *J. Appl. Phys.*, 70, 5932-34.

Corb B W, O'Handley R C (1985), "Magnetic properties and short-range order in Co–Nb–B alloys", *Phys. Rev. B*, 31(11), 7213–7219.

A. M. Ghemawat, M. E. McHenry, and R. C. O'Handley, "Magnetic moment suppression in rapidly solidified Co–TE–B alloys", *J. Appl. Phys*., 63, 3388–3390 (1989).

Friedel J (1958), "Theory of magnetism in transition metals", *Nuevo Cim. Suppl*., 7, 287.

O'Handley R C (1987), "Physics of ferromagnetic amorphous alloys", *J. Appl. Phys*., 62, R15.

Williams A R, Moruzzi V L, Malozemoff A P, Terakura K (1988), "Generalized Slater-Pauling curve for transition metal magnets", *IEEE Trans. Mag*., 19, 1983-88.

Nelson J B, Riley D P (1945), "An experimental investigation of extrapolation methods in the derivation of accurate unit-cell dimensions of crystals", *Proc. Phys. Soc*., 57, 160.

Cahn R W, Haasen P (1996), *Physical Metallurgy,* 4th ed., vol.1, North Holland, Amsterdam.

http://www.metalprices.com

http://www.metal-pages.com

Kurniawan M, Keylin V, McHenry M E (2015), "Alloy substituents for cost reduction in soft magnetic materials", *J. Mater. Res*., 30 (08), 1072-1077.

Kurniawan M, Keylin, V, McHenry M E (2015), "Effect of alloy substituents on soft magnetic properties and economics of Fe-based and Co-based alloys", *J. Mater. Res*., 30 (14), 2231-2237.

Belyea D D, Lucas M S, Michel E, Horwath J, Miller C W (2015), "Tunable magnetocaloric effect in transition metal alloys", *Sci. Rep.*, 5.

McHenry M E, Willard M A, Laughlin D E (1999), "Amorphous and nanocrystalline materials for applications as soft magnets", *Prog. Mat. Sci*., 44 (4), 291-433.

Ebert H, Kodderitzsch D, Minar J (2011), "Calculating condensed matter properties using the KKR-Green's function method – recent developments and applications", *Rep. Prog. Phys*., 74, 096501.

# Figures and Tables

This article has been accepted for publication in a future issue of this journal, but has not been fully edited. Content may change prior to final publication. Citation information: DOI 10.1109/LMAG.2016.2592462, IEEE Magnetics Letters

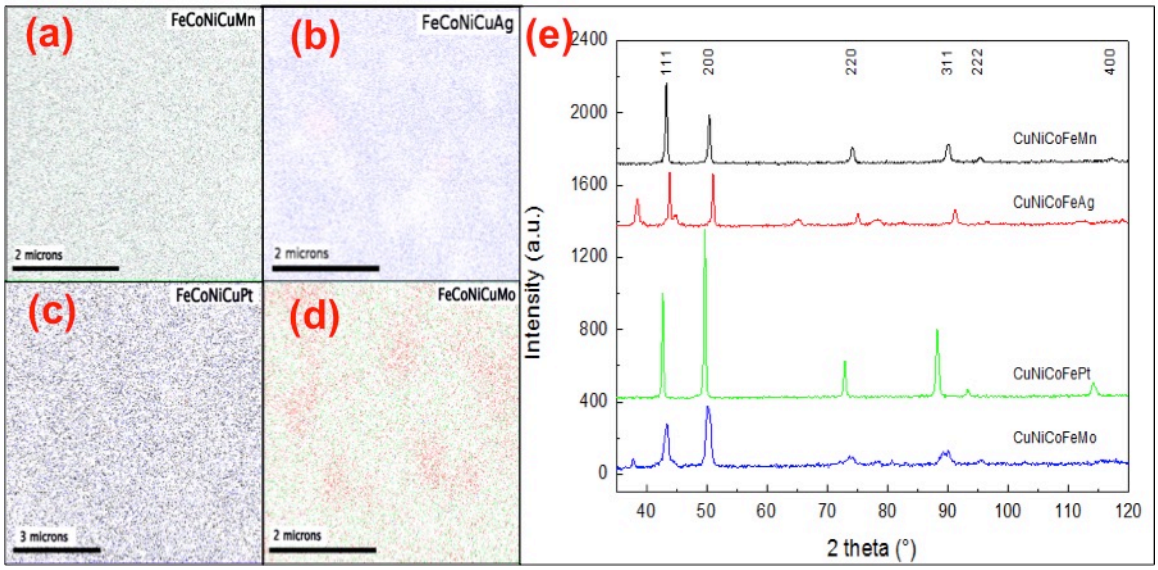


Fig. 1. Area scan EDS results of as-cast; (a) FeCoNiCuMn, (b) FeCoNiCuAg, (c) FeCoNiCuPt, and (d) FeCoNiCuMo. XRD patterns (e) of as-cast FeCoNiCuX (X=Mn, Ag, Pt, Mo) samples, indexed to Fm-3m peaks.

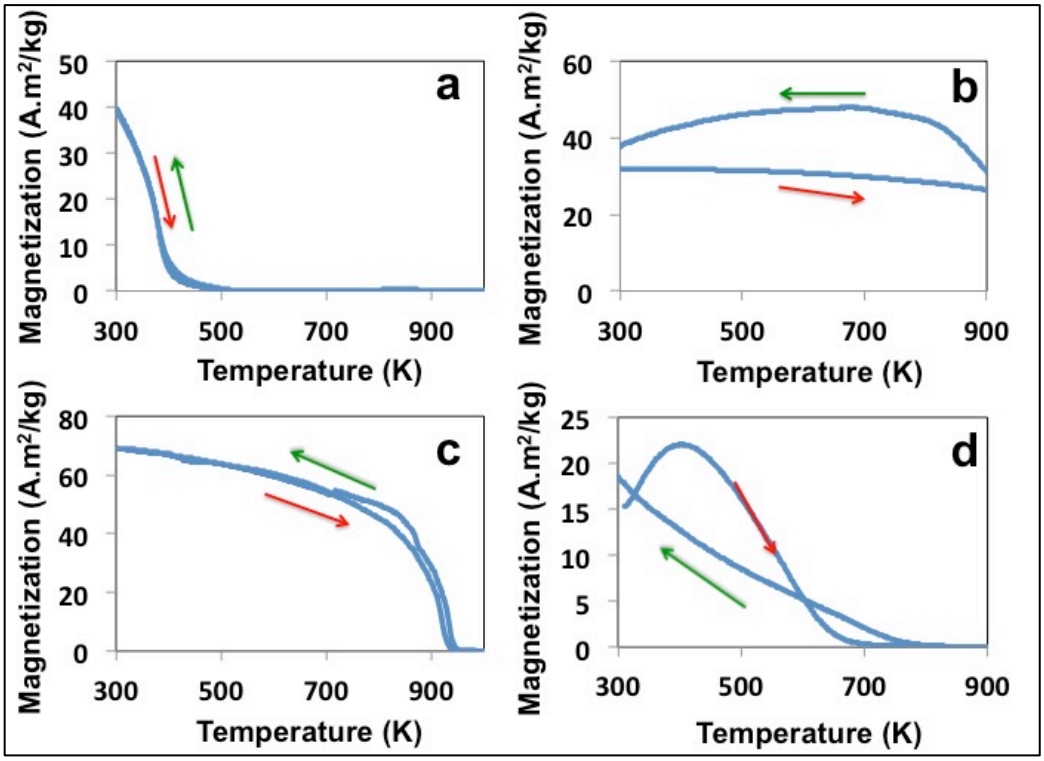


Fig. 2. Magnetization (M-T) curves for FeCoNiCuX (300 – 1000 K) for samples with X; (a) Mn, (b) Ag, (c) Pt, and (d) Mo. M-T during heating (red arrow) and cooling (green

This article has been accepted for publication in a future issue of this journal, but has not been fully edited. Content may change prior to final publication. Citation information: DOI 10.1109/LMAG.2016.2592462, IEEE Magnetics Letters

arrow) is shown here with complete reversibility observed in FeCoNiCuMn and FeCoNiCuPt. An applied field of 8.7 kA/m (100 Oe) was used for the M-T measurement.

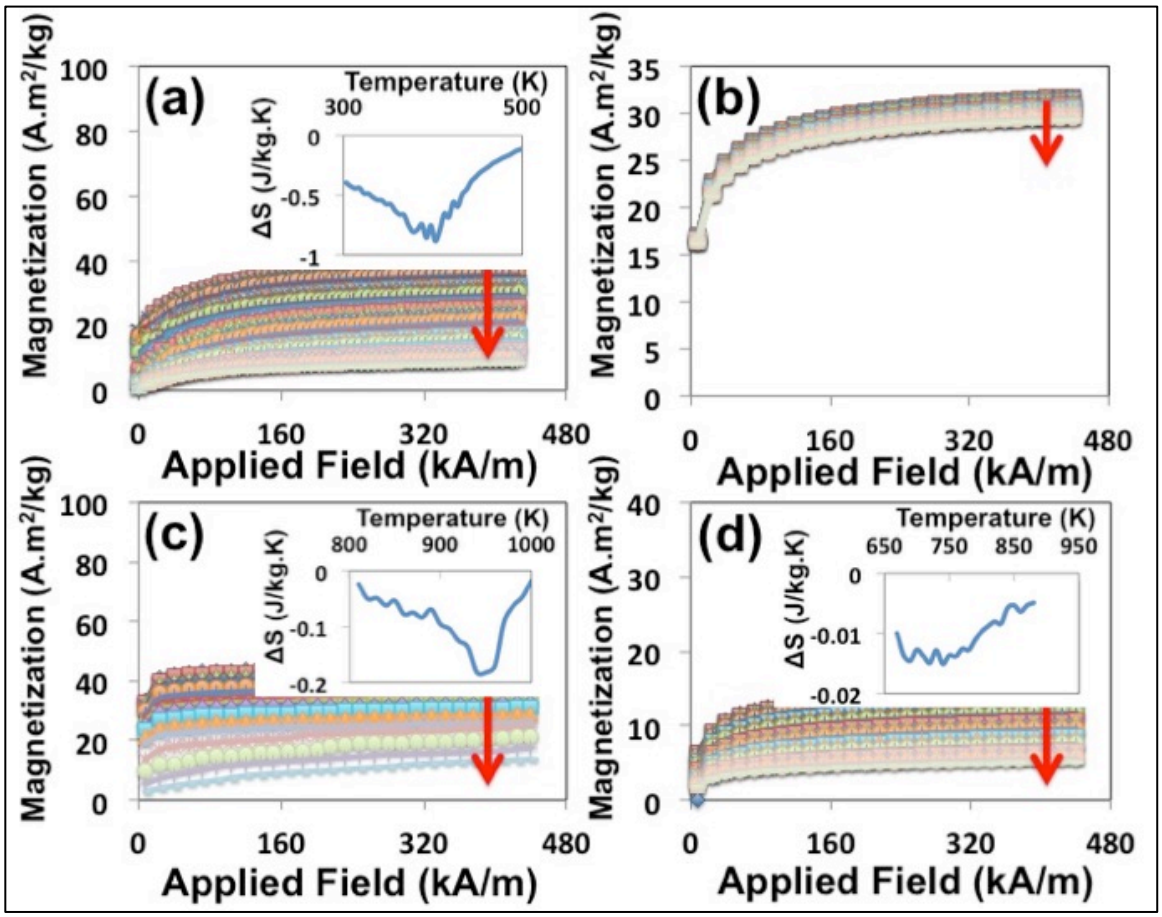


Fig. 3. Isothermal M-H curves of FeCoNiCuX near their $T_c$ (except FeCoNiCuAg). Red arrows are in the direction of increasing temperature. X for these 4 samples; (a) Mn, (b) Ag, (c) Pt, and (d) Mo. The insets are their respective ΔS–T curves for a maximum applied field of 480 kA/m (5500 Oe).

Table I. Configurational entropy of alloys with >5 components. Herein, we also consider configurational entropy in $FeCoNiCu_{1-x}Mn_{1+x}$ alloys with slight deviation from equiatomic composition. The expression $\Delta S_{config} = R \times \Sigma X_i \ ln(X_i)$ is used for this calculation.

| Cu % | Mn % | $S_{config}$ (arb.) | $\Delta S_{config}$ (%) |
|---|---|---|---|
| 20 | 20 | 13.381 | 0.000 |
| 19 | 21 | 13.377 | -0.031 |

This article has been accepted for publication in a future issue of this journal, but has not been fully edited. Content may change prior to final publication. Citation information: DOI 10.1109/LMAG.2016.2592462, IEEE Magnetics Letters

| Cu % | Mn % | $S_{config}$ (arb.) | $\Delta S_{config}$ (%) |
|---|---|---|---|
| 18 | 22 | 13.364 | -0.124 |
| 17 | 23 | 13.343 | -0.281 |
| 16 | 24 | 13.314 | -0.500 |
| 15 | 25 | 13.276 | -0.785 |
| 6 comp. (equiatomic) | 0.167 | 14.897 | 11.328 |
| 7 comp. (equiatomic) | 0.143 | 16.178 | 20.906 |

Table II. Comparison of measured and calculated $T_c$ of several equiatomic HEAs. The asterisk (*) denotes alloys with observed chemical partitioning based on the XRD and SEM analysis.

| | Calculated $T_c$ (K) | Measured $T_c$ (K) |
|---|---|---|
| FeCoNiCu | 1059 | >1000 |
| FeCoNiCuGa | 714 | 800 |
| FeCoNiCuAg* | 850 | >1000 |
| FeCoNiCuPt | 906 | 864 |
| FeCoNiCuMo* | 710 | 657 |
| FeCoNiCuMn | 414 | 400 |
| FeCoNiCuGaPt | 646 | 625 |
| FeCoNiCuMnPt | 316 | ? |

Table III. Comparison of measured and calculated $T_c$ of $FeCoNiCu_{1-x}Mn_{1+x}$ alloys.

| | Calculated $T_c$ (K) | Measured $T_c$ (K) |
|---|---|---|
| FeCoNiCuMn | 414 | 400 |
| $FeCoNiCu_{0.95}Mn_{1.05}$ | 392 | 280 |
| $FeCoNiCu_{0.90}Mn_{1.10}$ | 370 | 265 |

This article has been accepted for publication in a future issue of this journal, but has not been fully edited. Content may change prior to final publication. Citation information: DOI 10.1109/LMAG.2016.2592462, IEEE Magnetics Letters

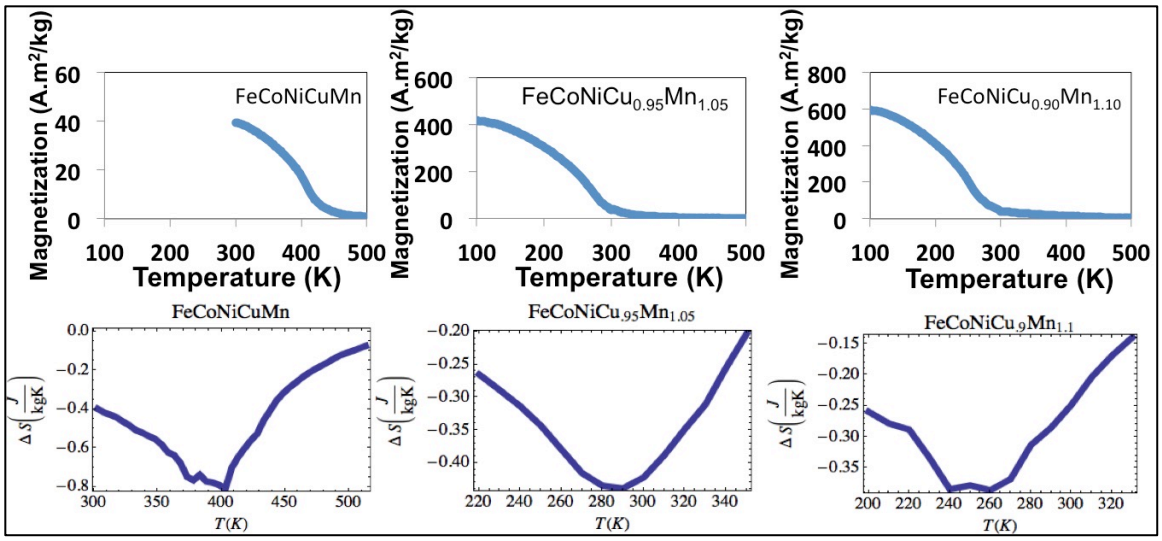


Fig. 4. M-T and ΔS–T (in $^{J}/_{kg.K}$) curves of $FeCoNiCu_{1+x}Mn_{1-x}$ alloys.